Raman scattering of longitudinal-optical-phonon-plasmon coupling in Cl-doped ZnSe under high pressure

Y. C. Lin, C. H. Chiu, W. C. Fan, C. H. Chia, S. L. Yang, D. S. Chuu, M. C. Lee, W. K. Chen, W. H. Chang, and W. C. Chou

Citation: Journal of Applied Physics **102**, 123510 (2007); doi: 10.1063/1.2826936
View online: http://dx.doi.org/10.1063/1.2826936
View Table of Contents: http://scitation.aip.org/content/aip/journal/jap/102/12?ver=pdfcov
Published by the AIP Publishing

Raman scattering of longitudinal-optical-phonon-plasmon coupling in Cl-doped ZnSe under high pressure

Y. C. Lin, C. H. Chiu, W. C. Fan, C. H. Chia, S. L. Yang, D. S. Chuu, M. C. Lee, W. K. Chen, W. H. Chang, and W. C. Chou[a)]
Department of Electrophysics, National Chiao Tung University, Hsinchu 30010, Taiwan, Republic of China

(Received 29 August 2007; accepted 24 October 2007; published online 26 December 2007)

The vibrational, electronic, and crystalline properties of *n*-type chlorine-doped ZnSe (ZnSe:Cl) layers with a carrier concentration from 8.2×10^{15} to 1.8×10^{18} cm^{-3} are studied by Raman spectroscopy. The spectral line shapes of the longitudinal-optical-phonon and plasmon coupling mode are analyzed using the Raman scattering efficiency and the dielectric function to obtain the electron densities and mobility. The splitting of the transverse-optical (TO) phonon and the redshift of the chlorine-related impurity vibration mode are clearly observed when pressure is applied. The semiconductor-to-metal phase transition pressure of ZnSe:Cl layers declines as the carrier concentration increases, indicating that *n*-type doping reduces crystal stability. Additionally, the pressure-induced weakening of the longitudinal-optical-phonon-plasmon coupling efficiency suggests that pressure tends to degrade the *n*-type characteristic of ZnSe:Cl because of the emergence of the new deep donorlike state. © *2007 American Institute of Physics*.
[DOI: 10.1063/1.2826936]

I. INTRODUCTION

Materials at high pressure exhibit interesting phenomena. For example, Mao *et al.* made optical measurements at ~250 GPa and observed that hydrogen becomes metallic due to a band overlap.[1] Water (H_2O) molecules under high pressure cleave and form O_2 and H_2 bonds.[2] Semiconductors at high pressure also exhibit fascinating behavior. Smith *et al.*[3] found that ZnSe undergoes a crystallographic phase transition from a fourfold coordination zinc blende (ZB) structure to a sixfold-coordinated rock-salt (RS) structure at about 13.5 GPa. Itkin *et al.* studied the sharp drop of resistance from 10^{21} to 10^4 Ω in ZnSe at 13.5 GPa,[4] which indicates that pressure-induced metallization of ZnSe occurs when the crystalline structure is transformed from ZB to RS. The high-pressure resistance measurement is consistent with the optical measurement, yielding a monotonic energy blueshift with pressure and an abrupt transformation to opaque at 13.5 GPa.[5] Our earlier studies investigated the physical properties of undoped ZnSe[6] and ZnSe-based ternary compounds, ZnMnSe,[7] ZnFeSe,[6] ZnCdSe,[8,9] and ZnSeTe,[10] at high pressure using energy-dispersive x-ray diffraction, Raman scattering, and photoluminescence measurements. The disappearance of the longitudinal-optical (LO) phonon at high pressure is caused by the metallization of the ZnSe-based ternary compounds.

Recently, longitudinal-optical-phonon and plasmon coupling (LOPC) was investigated using Raman scattering to characterize the hole concentration of GaMnAs.[11,12] The strong interaction between LO phonons and collective excitations (plasmons) via their associated macroscopic electric fields has also been extensively studied[13] in other compound semiconductors such as SiC, GaAs, and GaN.[14–16] According to related works, the free carrier concentration and mobility can be obtained by analyzing the line shapes of the measured Raman spectra. A question arises: based on the powerful high-pressure approach for tuning the physical properties of semiconductors, can the applied high pressure significantly alter the interesting LO phonon and plasmon coupling? The applied pressure modifies the vibration frequency of the LO phonon and the carrier concentration by contracting the lattice. A notable change in the LOPC under the applied high pressure might be expected. In particular, little attention has been paid to the LOPC of the II–VI semiconductors because of their low electron mobility and large plasmon damping. Furthermore, the pressure-induced semiconductor-to-metal phase transition and the crystal stability of *n*-type ZnSe:Cl layers, which are affected by the doping concentration, remain unexplored.

In this work, Raman scattering is adopted to investigate the LOPC as a function of applied pressure for *n*-type ZnSe:Cl layers. Based on the Raman scattering efficiency and the dielectric function, the spectral line shape is analyzed to obtain the free carrier concentration and mobility. Moreover, the semiconductor-to-metal phase transition of *n*-type ZnSe:Cl layers is studied.

II. EXPERIMENT

ZnSe:Cl layers were grown by molecular beam epitaxy on semi-insulating GaAs (001) substrates, which were chemically etched and thermally desorbed to remove residual oxide just prior to growth. The Cl beam was supplied *in situ* from a $ZnCl_2$ compound source, using the conventional effusion cell. The Cl-doping level was controlled by adjusting the $ZnCl_2$ effuse temperature (T_{Cl}). The substrate temperature was maintained at 300 °C, and the thickness of the

a)Author to whom correspondence should be addressed. Electronic mail: wuchingchou@mail.nctu.edu.tw.

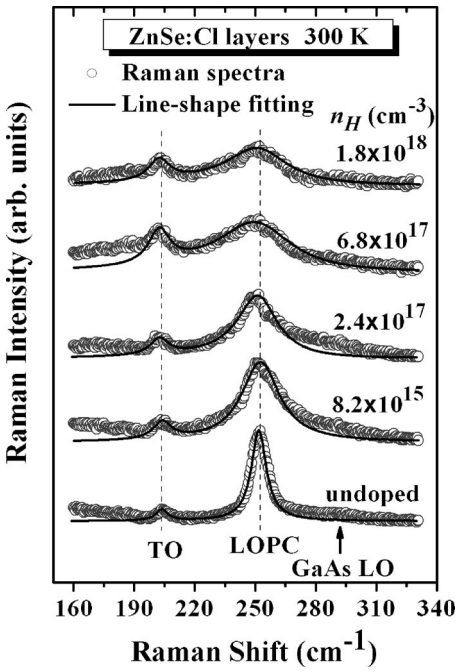

FIG. 1. Raman spectra (open circles) with calculated line shape analysis (solid lines) of *n*-type ZnSe:Cl layers for various carrier densities at 300 K and ambient pressure, including Lorentzian fit for the TO phonon.

ZnSe:Cl layers was fixed at about 0.9 μm. The samples were electrically characterized using conventional Hall measurements at room temperature (RT) in the Van der Pauw configuration. The undoped sample was highly resistive with carrier concentration of under 10^{15} cm^{-3} at RT and the net *n*-type carrier concentration from 8.2×10^{15} to 1.8×10^{18} cm^{-3} for T_{Cl} between 110 and 140 °C was discussed.

High-pressure measurements were made in a gasket diamond anvil cell (DAC). A methanol-ethanol 4:1 mixed liquid, loaded under high pressure, was used as a pressure-transmitting medium to maintain the hydrostatic conditions. The hydrostatic pressure was calibrated by the spectral shift of the ruby $R1$ line. The pressure gradient was less than 0.2 GPa, as determined by measurements made at various positions of the sample chamber. Before the ZnSe:Cl sample was loaded into the DAC, the GaAs substrate was removed by mechanical polishing and chemical etching.

Raman spectra were obtained at RT and collected in the backscattering configuration using a 514.5 nm line of an Ar^+-ion laser as the excitation source. The spectra were obtained using a SPEX 1404 double grating spectrometer equipped with a multichannel LN_2-cooled charge-coupled device. The reproducibility of the Raman peak frequencies was better than ±0.1 cm^{-1}. The photoluminescence (PL) spectra were obtained at RT, using the 325 nm line of a He-Cd laser, and detected with a photomultiplier tube.

III. RESULTS AND DISCUSSION

Figure 1 presents the Raman spectra of *n*-type ZnSe:Cl layers for various carrier concentration and an undoped ZnSe layer. The spectra were all obtained at room temperature and ambient pressure under $z(x+y,x+y)\bar{z}$ backscattering geometry. In this configuration, based on the selection rule, scattering from the LO phonon is allowed, while that from the transverse-optical (TO) phonon is forbidden. However, a weak TO feature, which appears at around 203.5 cm^{-1}, is attributable to a slight deviation from perfect backscattering geometry. As the carrier concentration increases from less than 10^{15} cm^{-3} (undoped) to 1.8×10^{18} cm^{-3} (T_{Cl} = 140 °C), the LO-phonon line shifts from 252.2 to 248.8 cm^{-1} due to coupling of the LO phonons and plasmons (LOPC). This LOPC mode behavior is characteristic of semiconductors with low carrier mobility or large plasmon damping. Therefore, only one overdamped phononlike LOPC mode near the LO phonon is observed, rather than two coupled LOPC modes.[11–13,17] Also, the linewidth, which is the full width at half maximum (FWHM), of the LOPC mode broadens from 10.4 to 25.6 cm^{-1}, and the peak intensity ratios ($I_{\mathrm{LOPC}}/I_{\mathrm{TO}}$), which are given in Table I, drop from 6.7 to 1.3. A line shape analysis of the LOPC mode is performed and displayed as solid lines in Fig. 1 to examine further the correlation between the vibrational and the electronic properties of *n*-type ZnSe:Cl for various carrier concentration. The line shape fitting analysis is based on the Raman efficiency and is given by[18]

$$I(\omega) = SA(\omega)\mathrm{Im}[-1/\varepsilon(\omega)], \tag{1}$$

where ω represents the Raman shift and S is an ω-independent proportionality constant. $A(\omega)$ is a coefficient given by

$$\begin{aligned} A(\omega) = 1 &+ 2C\omega_T^2[\omega_p^2\gamma(\omega_T^2-\omega^2) - \omega^2\Gamma(\omega^2+\gamma^2-\omega_p^2)]/\Delta \\ &+ C^2(\omega_T^2/\Delta)\{\omega_p^2[\gamma(\omega_L^2-\omega_T^2) + \Gamma(\omega_p^2-2\omega^2)] \\ &+ \omega^2\Gamma(\omega^2+\gamma^2)\}/(\omega_L^2-\omega_T^2), \end{aligned} \tag{2}$$

TABLE I. Hall carrier concentration (n_H) and mobility (μ_H), LOPC mode frequencies, linewidth (FWHM), and peak intensity ratio ($I_{\mathrm{LOPC}}/I_{\mathrm{TO}}$) of all studied ZnSe samples with various $ZnCl_2$ doping temperatures (T_{Cl}).

T_{Cl} (°C)	Hall concentration n_H (cm^{-3})	Hall mobility μ_H (cm^2/V s)	LOPC mode frequency (cm^{-1})	FWHM of LOPC mode (cm^{-1})	Intensity ratio ($I_{\mathrm{LOPC}}/I_{\mathrm{TO}}$)
Undoped	···	···	252.2[a]	10.4[a]	6.7[a]
110	8.2×10^{15}	154	251.3	19.8	5.2
120	2.4×10^{17}	141	250.5	24.4	3.0
130	6.8×10^{17}	106	249.2	25.3	1.3
140	1.8×10^{18}	67	248.8	25.6	1.3

[a]Phonon frequency, FWHM, and intensity ratio of undoped ZnSe LO phonon.

TABLE II. Carrier concentration (n_R), mobility (μ_R), and mobility ratios (μ_H/μ_R) obtained by optical Raman measurements. Plasmon frequency (ω_p), plasmon damping constant (γ), and phonon damping constant (Γ) are derived by the calculated line shape analysis.

				Fitting parameters		
T_{Cl} (°C)	Carrier concentration from Raman n_R (cm^{-3})	Mobility from Raman μ_R ($cm^2/V\,s$)	Mobility ratio (μ_H/μ_R)	ω_p (cm^{-1})	γ (cm^{-1})	Γ (cm^{-1})
110	7.3×10^{15}	76	2.0	26	770	23
120	2.1×10^{17}	45	3.1	140	1300	29
130	4.8×10^{17}	32	3.3	210	1800	50
140	7.1×10^{17}	20	3.4	255	2890	53

$$\Delta = \omega_p^2\gamma[(\omega_T^2-\omega^2)^2+(\omega\Gamma)^2]+\omega^2\Gamma(\omega_L^2-\omega_T^2)(\omega^2+\gamma^2). \tag{3}$$

Here, the dimensionless Faust–Henry coefficient (C) can be deduced from the intensity ratio of LO and TO phonon peaks from an undoped ZnSe layer[19]

$$\frac{I_{LO}}{I_{TO}} = \left(\frac{\omega_I-\omega_L}{\omega_I-\omega_T}\right)^4\frac{\omega_T}{\omega_L}\left(1+\frac{\omega_T^2-\omega_L^2}{C\omega_T^2}\right)^2. \tag{4}$$

In Eq. (4), ω_I is the incident photon frequency. The Faust–Henry coefficient used in the analysis is $C=-0.21$. The dielectric function with the plasmon damping term (γ) is given by

$$\varepsilon(\omega) = \varepsilon_\infty\left(1+\frac{\omega_L^2-\omega_T^2}{\omega_T^2-\omega^2-i\omega\Gamma}-\frac{\omega_p^2}{\omega^2-i\omega\gamma}\right), \tag{5}$$

where ε_∞ is the high-frequency dielectric constant; $\omega_L(\omega_T)$ are the LO (TO) phonon frequencies of undoped ZnSe; Γ is the phonon damping constant, and ω_P is the plasmon frequency,

$$\omega_p^2 = \frac{4\pi ne^2}{\varepsilon_\infty m^*}, \tag{6}$$

where m^* is an electron effective mass.

Hence, the free electron density, n, can be estimated using Eq. (6) with line shape analysis. Table II gives the fitting parameters and $\gamma > \omega_P$ is clearly observed, revealing that the plasmon is overdamped. The overdamped plasmon strongly influences the linewidth of the LOPC mode and yields only one observable phononlike mode.[13,17]

Table II presents the carrier concentration obtained from Raman (n_R) measurements at 300 K as a function of $ZnCl_2$ effusion cell temperature. Figure 2 plots the carrier concentrations obtained from the Hall (n_H) and Raman (n_R) measurements. The figure demonstrates that the carrier concentration obtained from the two methods agree closely, revealing that the Raman scattering is an effective and nondestructive approach for determining the free carrier density in n-type ZnSe:Cl layers. The slight deviation between these two experimental results has several causes. First, the GaAs TO phonon near the high-frequency side of the LOPC mode may influence the accuracy of the line shape fitting. Second, the Cl-related impurity mode, which is only clearly identified at high pressure appears at the low frequency side of LOPC and will be discussed later. However, it may slightly affect the line shape analysis. Finally, $m^*=0.16m_0$ and $\varepsilon_\infty=6.1$,[20] were used in Eq. (6) to calculate the free carrier density. Because of the polaron effect,[21] it is rather difficult to determine the electron effective mass properly. The possible values of electron concentration and mobility calculated by using different values of effective mass and dielectrics were expressed by the error bars in Figs. 2 and 3.

Figure 3 compares the mobility obtained from the Hall measurements (μ_H) and the line shape analysis of Raman spectra (μ_R) using the equation $\mu_R=e/m^*\gamma$. The mobility ratio (μ_H/μ_R) is between 2.0 and 3.4, depending on the elec-

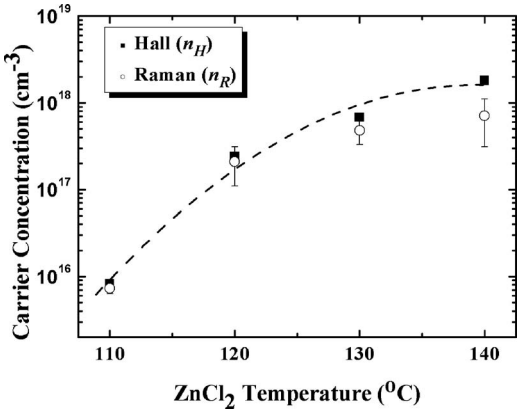

FIG. 2. Carrier concentration obtained at 300 K from Hall measurement n_H (full squares), compared with those obtained from optical Raman measurement n_R (open circles), as a function of the $ZnCl_2$ source temperature. The dashed line is merely a guide for the eye.

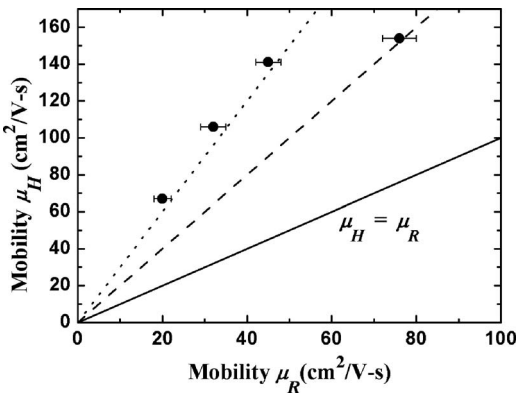

FIG. 3. Mobility obtained at 300 K from Hall measurement μ_H vs those obtained from optical Raman measurement μ_R. The solid, dashed, and dotted lines, respectively, represent the ratio, $\mu_H/\mu_R=1$, 2, and 3.

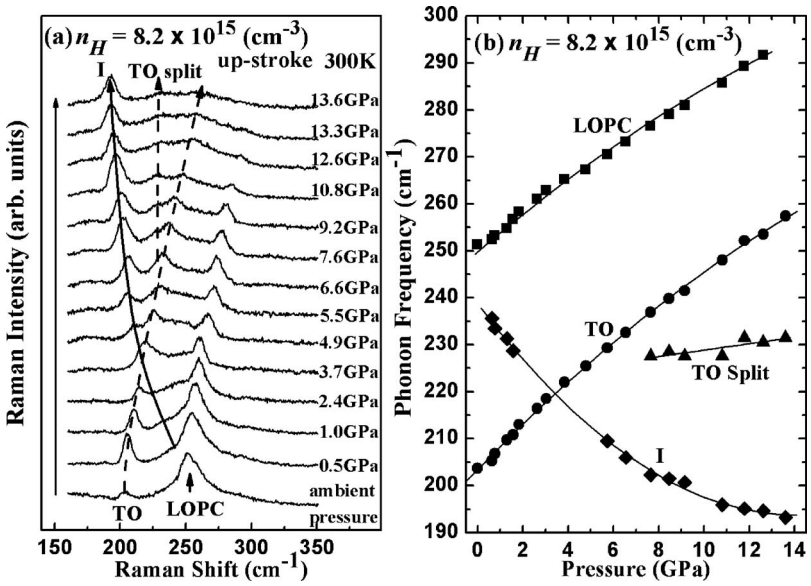

FIG. 4. (a) Up-stroke pressure-dependent Raman spectra of the ZnSe:Cl layer (n_H=8.2×10^{15} cm^{-3}) at 300 K. The behavior of mode *I* and the TO phonon are indicated by solid and dotted arrows, respectively. (b) Pressure dependence of Raman shifts for LO, TO, TO split, and mode *I* of the ZnSe:Cl layer (n_H=8.2×10^{15} cm^{-3}). The solid curves are quadratic polynomial fits.

tron concentration. Similar experimental results were reported in *p*-type GaAs with lower mobility. For instance, Fukasawa *et al.*,[22] Gargouri *et al.*,[23] Mlayah *et al.*,[24] and Irmer *et al.*,[25] respectively, obtained $\mu_H/\mu_R \approx 1.5-2.6$, 3.7, 2.0, and 2.3. The difference between μ_H (Hall mobility) and μ_R (optical Raman mobility) is reasonable because the optical Raman mobility is calculated from the plasmon damping due to individual excitation, while the Hall mobility originates from electron scattering with phonons and ionized impurities.

Figure 4(a) shows the up-stroke pressure-dependent Raman spectra of *n*-type ZnSe:Cl layer (8.2×10^{15} cm^{-3}) at room temperature. The applied pressure reduces the lattice constant and the crystal volume, shifting the LOPC and TO phonons to higher frequencies, accompanied with a decrease in intensity. As presented in Fig. 4(a), the TO phonon splits into two peaks at 7.6±0.3 GPa and the peaks depend differently on pressure. Investigations of nonmagnetic and magnetic II–VI ternary compounds have shown that pressure-induced TO phonon splitting contributes to the formation of an additional (cinnabar) phase.[6,7,10] Furthermore, a weak feature, which is assigned to a Cl-related impurity mode (*I*), appears at the low-frequency side of the LOPC mode. As the pressure increases, this phonon mode tends to exhibit negative dependence on pressure and becomes more intense. At 3.0±0.3 GPa, the *I* mode overlaps with the TO phonon. As the pressure increases further, the two modes cross each other. Figure 4(b) plots the Raman-shift versus the pressure of all of the phonon modes, with quadratic polynomial fitting. The LO phonon disappears and the sample becomes opaque at 13.6±0.2 GPa. These facts are evidence of the semiconductor-to-metal phase transition. The transition pressure, which is almost identical to that of the undoped binary ZnSe crystals,[9,10] can be attributed to the lower doping concentration. However, two TO phonon modes and the *I* mode are still observed in the Raman spectra when the semiconductor-to-metal phase transition occurs because the Cl-related and TO modes are transverse vibration modes and can exist on the surface of metal even if the depth of penetration by the excitation laser beam into the metal is merely several tens of angstroms.[6,9]

Figure 5(a) displays the up-stroke pressure-dependent Raman spectra of ZnSe:Cl layer (1.8×10^{18} cm^{-3}). Figure 5(b) summarizes all of the phonon modes. As can be seen in Fig. 5(a), the Cl-related impurity mode (*I*) is more clearly identified than that of the samples with lower concentration. The mode *I* and the TO phonon are found to overlap at 3.4±0.3 GPa. Additionally, at 7.6±0.4 GPa, pressure-induced TO phonon splitting is observed. However, as the applied pressure is increased to 12.5±0.1 GPa, the LO phonon disappears and the sample becomes opaque. The semiconductor-to-metal phase transition pressure is lower, 12.5 GPa, than that of the sample with the lower concentration (8.2×10^{15} cm^{-3}), 13.6 GPa, discussed earlier.

Figure 6 plots the phase transition pressure versus the carrier concentration of all studied ZnSe:Cl layers. As the carrier concentration is increased from 8.2×10^{15} to 1.8×10^{18} cm^{-3}, the phase transition pressure falls from 13.6 to 12.5 GPa, indicating that *n*-type doping tends to reduce the stability of the crystal. The inset in Fig. 6 presents the PL spectra of all samples excited by the 325 nm line of a He-Cd laser at room temperature, to understand the source of the decrease in the phase transition pressure as carrier concentration increases. The sharp peak at 2.68 eV is the near band edge emission, arising from a Cl_{Se} donor to valence band transition. The broad midgap band in the 1.8 to 2.4 eV range is typically assigned to the donor-to-acceptor pair recombination or self-activated (SA) emission.[26] The SA emission is caused by recombination from the intentional shallow donor (Cl_{Se}) to the deep acceptor state (zinc vacancy). The oscillations are interference fringes associated with the thin-film nature of the specimens. As the carrier concentration increases, the SA emission becomes more pronounced: the density of shallow donor (Cl_{Se}) and deep acceptor state (zinc vacancy) pairs increases. Such a crystal defect serves as the nucleation sites for the structural phase transition. This result corroborates the work of Pöykkö *et al.*,[27] who found that

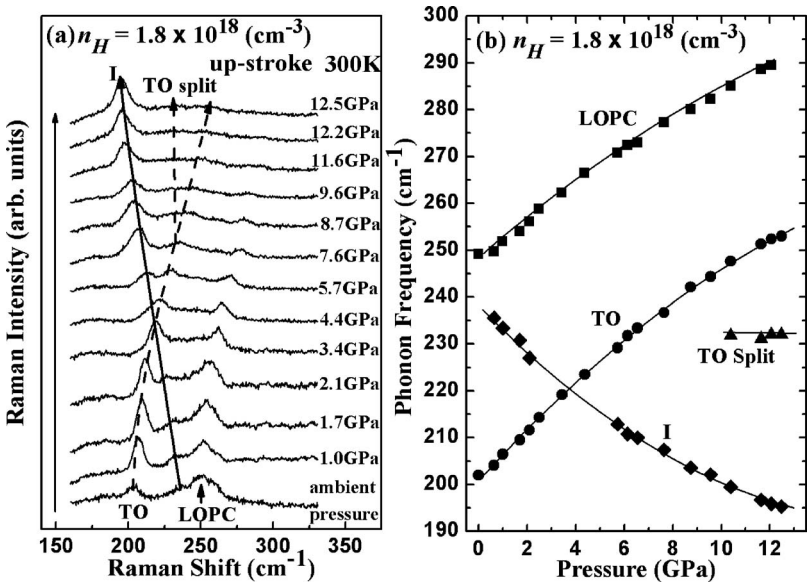

FIG. 5. (a) Up-stroke pressure-dependent Raman spectra of the ZnSe:Cl layer (n_H=1.8×10^{18} cm^{-3}) at 300 K. The LO phonon disappears at about 12.5 GPa. (b) Pressure-dependent Raman shifts of the ZnSe:Cl layer (n_H=1.8×10^{18} cm^{-3}). The solid curves represent quadratic polynomial fits.

defect complexes that are formed by Cl-impurity atoms and the native defects in ZnSe soften the lattice by producing large distortions. Muratov *et al.*[28] claimed that the zinc vacancies in ZnSe result in large lattice relaxation and alter the overall symmetry of a ZnSe crystal because of the relative shift in the distances of the first and second neighboring atoms from each vacancy. Therefore, the Cl donor and zinc vacancy pairs in *n*-type ZnSe:Cl layers are very likely to reduce the crystalline stability and the semiconductor-to-metal phase transition pressure.

Figure 7 plots the dependence of undoped ZnSe LO phonon and ZnSe:Cl (n_H=8.2×10^{15} cm^{-3} and 1.8×10^{18} cm^{-3}) LOPC mode frequencies on pressure to further elucidate the pressure-dependent LOPC mode of *n*-type ZnSe:Cl layers. The solid curve shows a quadratic polynomial fit to the undoped ZnSe LO phonon results and the dashed line displays the same fitting curve but shifted downward to capture the assumed behavior of the LOPC mode of ZnSe:Cl (n_H=1.8×10^{18} cm^{-3}) under pressure. Apparently, when the applied pressure is less than 2.5–3.0 GPa, the behavior of the LOPC mode of ZnSe:Cl (n_H=1.8×10^{18} cm^{-3}) follows the dashed curve. However, it deviates and turns to follow undoped behavior as the pressure increases further. Similar results are observed for other samples with different carrier concentration. Moreover, as the carrier density increases, this behavior becomes pronounced. In addition to the blueshift of the LOPC mode, the decline in the FWHM in the LOPC mode when pressure is applied (inset in Fig. 7) is also a signature of a decreasing in electron concentration, as discussed in Fig.

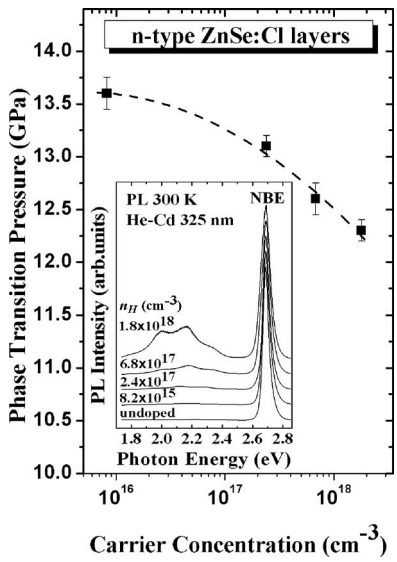

FIG. 6. Carrier concentration (n_H)-dependent phase transition (semiconductor-to-metal) pressure of the *n*-type ZnSe:Cl layers. The dashed curve represents a quadratic polynomial fit. The inset displays the PL spectra of undoped ZnSe and the *n*-type ZnSe:Cl layers at 300 K, excited by a He-Cd 325 nm laser.

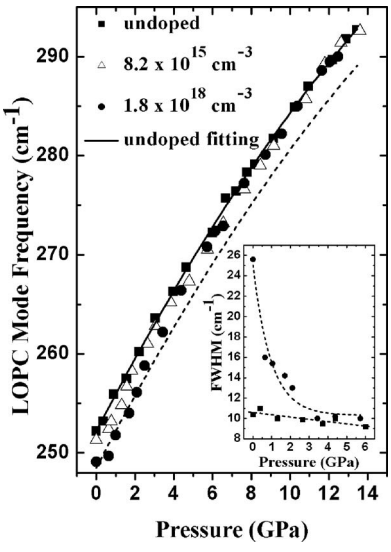

FIG. 7. Pressure-dependent LO phonon of undoped ZnSe (full squares) and the LOPC mode of *n*-type ZnSe:Cl for n_H=8.2×10^{15} cm^{-3} (open triangles) and n_H=1.8×10^{18} cm^{-3} (full circles). The solid curve is a quadratic polynomial fit of an undoped ZnSe LO phonon and the dashed curve is the same curve but shifted downward to capture the presumed behavior of the LOPC mode of ZnSe:Cl (n_H=1.8×10^{18} cm^{-3}). The inset plots the pressure-dependent FWHM of the undoped ZnSe LO phonon and the ZnSe:Cl LOPC mode (n_H=1.8×10^{18} cm^{-3}).

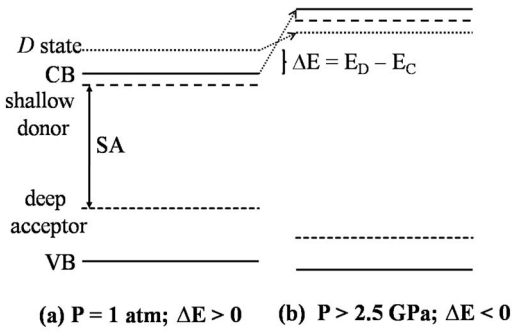

FIG. 8. Schematic band structure of *n*-type ZnSe:Cl. (a) At ambient pressure, the energy difference between the *D* state and the conduction band minimum, $\Delta E(E_D - E_C)$, is positive. (b) With compression, $\Delta E(E_D - E_C)$ declines and eventually becomes negative.

1. This behavior could also be associated with the pressure-induced weakening of LO-phonon-plasmon coupling that is caused by the fall in electron concentration.

Photoluminescence measurements made by Ritter *et al.* also revealed the degradation of *n*-type behavior in ZnSe at high pressure.[26] They indicated that applied hydrostatic pressure destabilizes the deep acceptor ground state of the zinc-vacancies-donor complexes and cause a new deep donorlike state (*D*) to enter the band gap of *n*-type ZnSe, modifying the rate of pressure shift of the SA emission, and degrading the *n*-type behavior of *n*-type ZnSe. Ritter *et al.*[26] concluded that the *D* state, which is located at 0.15–0.18 eV above the conduction band edge (CBE) at ambient pressure (Fig. 8), is very likely to be an excited state of the zinc-vacancies-donor complex. The pressure at which the LOPC mode deviates and turns to follow the undoped LO phonon is identical to the change in pressure of the SA emission in Ref. 26. Accordingly, the pressure-induced weakening of LO-phonon-plasmon coupling can be interpreted as being related to the emergence of the new deep donorlike state. The *D* state exhibits a much weaker dependence on pressure than the CBE.[26] Consequently, the energy difference between the *D* state and the conduction band minimum (at Γ point), $\Delta E(E_D - E_C)$, varies with the applied pressure. As can be seen in Fig. 8, ΔE is positive at ambient pressure. Under compression, ΔE decreases and eventually becomes negative. As ΔE becomes negative at about 2.5–3.0 GPa, the *D* state becomes entirely trapped with the transfer of electrons from the conduction band, degrading the *n*-type behavior of ZnSe:Cl, and reducing the LO-phonon-plasmon coupling efficiency.

IV. CONCLUSIONS

This work studied the vibrational, electronic, and crystalline properties of *n*-type ZnSe:Cl layers with carrier concentration from 8.2×10^{15} cm^{-3} to 1.8×10^{18} cm^{-3} using Raman spectroscopy. The spectra are well modeled by taking into account the phononlike coupled mode of the electron plasmons and the LO phonon. The Raman scattering efficiency and the dielectric function were calculated for the spectral line shape fittings. Carrier concentration obtained from the Hall and optical Raman measurements agree well. The semiconductor-to-metal phase transition pressure of *n*-type ZnSe:Cl layer declines as the carrier concentration increases. As the carrier concentration increases from 8.2×10^{15} to 1.8×10^{18} cm^{-3}, the phase transition pressure falls from 13.6 to 12.5 GPa, suggesting that *n*-type doping tends to reduce structural stability. Additionally, high-pressure Raman measurements revealed degradation of *n*-type behavior in ZnSe under compression. This behavior is attributable to the emergence of deep donorlike states.

ACKNOWLEDGMENTS

This work was supported by MOE-ATU and the National Science Council of Taiwan under Grant Nos. NSC 95-2112-M-009-047 and NSC 96-2112-M-009-026-MY3.

[1] H. K. Mao and R. J. Hemley, Science **244**, 1462 (1989).
[2] W. L. Mao, H. K. Mao, Y. Meng, P. J. Eng, M. Y. Hu, P. Chow, Y. Q. Cai, J. Shu, and R. J. Hemley, Science **314**, 636 (2006).
[3] P. L. Smith and J. E. Martin, Phys. Lett. **19**, 541 (1965).
[4] G. Itkin, G. R. Hearne, E. Sterer, M. P. Pasternak, and W. Potzel, Phys. Rev. B **51**, 3195 (1995).
[5] S. Ves, K. Strössner, N. E. Christensen, C. K. Kim, and M. Cardona, Solid State Commun. **56**, 479 (1985).
[6] C. M. Lin, D. S. Chuu, T. J. Yang, W. C. Chou, J. Xu, and E. Huang, Phys. Rev. B **55**, 13641 (1997).
[7] C. S. Yang, C. S. Ro, W. C. Chou, C. M. Lin, D. S. Chuu, J. Hu, E. Huang, and J. Xu, J. Appl. Phys. **85**, 8092 (1999).
[8] C. M. Lin, D. S. Chuu, J. Xu, E. Huang, W. C. Chou, J. Z. Hu, and J. H. Pei, Phys. Rev. B **58**, 16 (1998).
[9] Y. C. Lin, C. H. Chiu, W. C. Fan, S. L. Yang, D. S. Chuu, and W. C. Chou, J. Appl. Phys. **101**, 073507 (2007).
[10] C. S. Yang, W. C. Chou, D. M. Chen, C. S. Ro, J. L. Shen, and T. R. Yang, Phys. Rev. B **59**, 8128 (1999).
[11] M. J. Seong, S. H. Chun, H. M. Cheong, N. Samarth, and A. Mascarenhas, Phys. Rev. B **66**, 033202 (2002).
[12] W. Limmer, M. Glunk, S. Mascheck, A. Koeder, D. Klarer, W. Schoch, K. Thonke, R. Sauer, and A. Waag, Phys. Rev. B **66**, 205209 (2002).
[13] G. Abstreiter, M. Cardona, and A. Pinczuck, in *Light Scattering in Solids IV*, edited by M. Cardona and G. Güntherodt (Springer, Berlin, 1984), p. 5, and references therein.
[14] H. Harima, S. Nakashima, and T. Uemura, J. Appl. Phys. **78**, 1996 (1995).
[15] A. Mooradian and G. B. Wright, Phys. Rev. Lett. **16**, 999 (1966).
[16] T. Kozawa, T. Kachi, H. Kano, Y. Taga, and M. Hashimoto, J. Appl. Phys. **75**, 1098 (1994).
[17] G. Irmer, M. Wenzel, and J. Monecke, Phys. Rev. B **56**, 9524 (1997).
[18] M. V. Klein, B. N. Ganguly, and P. J. Colwell, Phys. Rev. B **6**, 2380 (1972).
[19] W. L. Faust and C. H. Henry, Phys. Rev. Lett. **17**, 1265 (1966).
[20] H. Hartmann, R. Mach, and B. Selle, in *Current Topics in Materials Science*, edited by E. Kaldis (North-Holland, Amsterdam, 1982), Vol. 9, p. 1, and references therein.
[21] D. M. Larsen, in *Polarons in Ionic Crystals and Polar Semiconductors*, edited by J. T. Devreese (North-Holland, Amsterdam, 1972), Chap. III.
[22] R. Fukasawa and S. Perkowitz, Phys. Rev. B **50**, 14119 (1994).
[23] M. Gargouri, B. Prevot, and C. Schwab, J. Appl. Phys. **62**, 3902 (1987).
[24] A. Mlayah, R. Carles, G. Landa, E. Bedel, and A. Muñoz-Yagüe, J. Appl. Phys. **69**, 4064 (1991).
[25] G. Irmer, J. Monecke, W. Siegel, G. Kühnel, B. H. Bairamov, and V. V. Toporov, in *Proceedings of the 13th International Conference on Raman Spectroscopy*, edited by W. Kiefer, M. Cardona, G. Schaack, F. W. Schneider, and H. W. Schrötter (Wiley, Chichester, 1992).
[26] T. M. Ritter, B. A. Weinstein, R. M. Park, and M. C. Tamargo, Phys. Rev. Lett. **76**, 964 (1996).
[27] S. Pöykkö, M. J. Puska, and R. M. Nieminen, Phys. Rev. B **57**, 12164 (1998).
[28] L. Muratov, S. Little, Y. Yang, B. R. Cooper, T. H. Myers, and J. M. Wills, Phys. Rev. B **64**, 035206 (2001).